BMC Veterinary Research

RESEARCH

Open Access

Toxicological screening of zinc oxide nanoparticles in mongrel dogs after seven days of repeated subcutaneous injections

Marwa H. Hassan[1,2], Ibrahim A. Emam[2], Haitham Farghali[2], Marwa A Ibrahim[3], Neven H. Hassan[4], Khaled Y. Farroh[5] and Eman I. Hassanen[6*]

Abstract

Zinc oxide nanoparticles (ZnO NPs) have recently been applied in various veterinary and medical fields, however, the toxicological evaluations of these NPs in dogs are lacking. Therefore, the current study is designed to assess the impact of exposure to daily subcutaneous (SC) injections of ZnO NPs at different concentrations on various organs of mongrel dogs. Nine dogs were randomly divided into three groups ($n=3$ for each) as follows: group (1) served as the control group, whereas groups (2&3) received SC injections of 50 and 100 ppm ZnO NPs (8 and 16 µg/kg bwt), respectively, once/day for 7 days. Our results revealed that ZnO NPs disrupted the oxidant/antioxidant balance in the lungs, liver, and kidneys of dogs in a dose-dependent manner. ZnO NPs induced dose-dependent radiological, ultrasonographical, and histopathological alterations in various organs especially lungs, spleen, liver, and kidneys along with disturbance in both liver and kidney biomarkers levels. Most organs of both ZnO NPs receiving groups displayed strong caspase-3 protein expression. Additionally, it upregulates the transcriptase levels of TNF-α and VEGF, as well as downregulates the antiapoptotic gene IL-10 in lung, kidney, and liver tissue homogenates. It was concluded that the daily SC injections of dogs with ZnO NPs at concentrations of 50 and 100 ppm caused extensive oxidative stress damage in various organs which provoked serious pathological processes such as apoptosis and inflammation.

Keywords Gene expression, Oxidative stress, Pathology, Ultrasonography, ZnO NPs

Introduction

Nanotechnology is the process of manipulating the shape and size of structures, electronics, and systems at the nanometer scale [1, 2]. Nanoparticles (NPs) with nanometer regions sized from 1 to 100 nm show exceptional characteristics because of their high surface area to volume ratio and diminutive size compared with macro-sized particles [3, 4]. They have been implanted in plentiful novel industrial branches such as pharmaceutical, chemical, mechanical, and food processing, moreover optics branches, drug delivery, medicinal techniques, and environmental sciences [5]. These NPs have

*Correspondence:
Eman I. Hassanen
eme_amr@cu.edu.eg; eme_amr@hotmail.com
[1]Department of Veterinary Clinical Sciences, Faculty of Veterinary Medicine, Jordan University of Science and Technology, Irbid, Jordan
[2]Department of Surgery, Anesthesiology and Radiology, Faculty of Veterinary Medicine, Cairo University, Giza, Egypt
[3]Department of Biochemistry and Molecular Biology, Faculty of Veterinary Medicine, Cairo University, Giza, Egypt
[4]Department of Physiology, Faculty of Veterinary Medicine, Cairo University, Giza, Egypt
[5]Nanotechnology and Advanced Materials Central Lab, Agricultural Research Center, Giza, Egypt
[6]Department of Pathology, Faculty of Veterinary Medicine, Cairo University, P.O. Box 12211, Giza, Egypt

the dimensions that make them suitable candidates for nanoengineering [6, 7].

Zinc oxide nanoparticles (ZnO NPs) are among the most significant metal oxide NPs due to their several key properties, including intense ultraviolet (UV) and infrared (IR) adsorption, strong catalytic activity, physical and chemical stability, and potent antibacterial activity [8]. Because nanosized particles can interact with the bacterial surface and/or the bacterial core once they enter the cell, they exhibit different bactericidal processes and have considerable antibacterial activity against a wide range of bacterial species [9–11]. ZnO NPs have been utilized for feed additives, food preservatives, and tissue repair [12]. ZnO NPs are broadly utilized in veterinary fields because of their potent antimicrobial, antineoplastic, and angiogenic activity [12]. They have been used to treat various skin lesions, such as infected wounds, eczema, dermatitis, and hemorrhoids in various animal species [13]. Recently, few studies revealed the ability of ZnO nanoparticles alone or in combination with other nanomaterials to accelerate the process of wound healing in dogs [14, 15]. Another study investigated the beneficial effect of Zn-containing drugs against canine atopic dermatitis [16]. Additionally, a further study determined the antifungal potential of ZnO NPs against *Microsporum canis* that was isolated from dogs and therefore, they recommend using ZnO NPs as an antimicrobial therapy for dermatophytes-mediated skin lesions in dogs after evaluating its safety in dogs [17]. Many reserchers validated that the direct topical application of ZnO NPs either alone or with antifungal agent for 14 days is markedly reduced the skin lesions of *Malassezia* and other fungal infections in dogs [18, 19].

The features that offer a promising opportunity for the creation of novel technologies in the medical field come with an unidentified risk to the welfare of animals and environmental safety. Besides the extensive uses of ZnO NPs, unknown risks could be created and most of them related to various cellular oxidative stress [20]. Mitochondrial malfunction, oxidative stress, and loss of cell viability are caused by changes in cellular zinc homeostasis [21]. Unexpected increases in free Zn^{2+} levels have the potential to damage lysosomes, releasing their contents into the cytoplasm and leading to cell death [22]. Many factors influencing ZnO NPs toxicity, including NPs size, concentration, route of administration, and frequency of exposure as well as animal species and breeding also control the pathological changes related to ZnO NPs [23, 24]. One study investigated the hepatotoxic effect of ZnO NPs in dogs after repeated oral administration that attributed to the oxidative stress damage [25].

Despite increasing the medicinal application of ZnO NPs, the potential toxicity of these metal oxide NPs is still sparse in various animal species, including dogs. It is important to investigate the toxicological effects of ZnO NPs at different concentrations via different routes to maintain their medicinal uses and reduce unfavorable adverse impacts. For this reason, the goal of the current study is to assess the possible systemic toxicity of different concentrations of ZnO NPs after 7-days of repeated subcutaneous injections in mongrel dogs. In addition, we explored the potential mechanism of such toxicity with a comprehensive insight into the molecular mechanisms.

Materials and methods

Preparation and characterization of zinc oxide nanoparticles (ZnO NPs)

In accordance with Kumar et al. [26], the precipitation process was used to create ZnO NPs. In a typical method, 50 ml of deionized water (Milli-Q, Millipore, USA) were used to dissolve 7.1883 g of zinc sulphate heptahydrate ($ZnSO4 \cdot 7H2O$, 99% purity, Sigma-Aldrich, USA). Next, sodium hydroxide (50 mL, 1 M) (98% purity, Sigma-Aldrich, USA) was added dropwise during magnetic stirring. Following the addition, the stirring was conducted for a further 30 min. Multiple rounds of pure water were used to filter and wash the precipitates. The precipitates were then dried at 60 °C for 24 h and calcined at 500 °C for two hours.

Two distinct examinations were performed on a powder of zinc oxide in the nano-size range. The chemical structures of the prepared NPs were evaluated using XRD technique. In the scanning mode of an X-ray diffractometer (X 'pert PRO, PAN analytical, Netherlands) using a Cu K radiation tube (=1.54 A) operating at 40 kV and 30 mA, the appropriate XRD pattern was captured. The standard ICCD library built into the PDF4 software was used to analyze the acquired diffraction pattern. The actual morphology of the as-prepared ZnO NPs was imaged by a High-Resolution Transmission Electron Microscope (HR-TEM) operating at an accelerating voltage of 200 kV (Tecnai G2, FEI, Netherlands). Diluted ZnO NPs solution was ultra-sonicated for 5 min to reduce the particle aggregation. Using a micropipette, three drops from the sonicated solution were deposited on a carbon-coated coated copper grid and left to dry at room temperature. HR-TEM images of the ZnO NPs that were deposited on the grid were captured for morphological evaluation.

Experimental animals

The current investigation was designed following the ARRIVE guidelines (PLoS Bio 8(6), e1000412,2010), and conducted after the approval of the Institutional Animal Care and Use Committee of Cairo University (IACUC), CU/F/40/23.

Nine healthy male mongrel dogs of different ages (1–1½ years), weighing (15–20 kg), were obtained from

dogs' owners to be enrolled in the present study. All dogs' owners were aware that their animals will be included in research purposes and signed a written consent indicating their approval. The Power Calculation Method was used for sample size calculation as we calculated the sample size on SPSS version 18.0 software (SPSS Inc, Chicago, IL., USA) using Paired t-test http://www.biomath.info/power/prt.htm. Dogs were housed individually at the kennels of the Department of Surgery, Anesthesiology and Radiology, Faculty of Veterinary Medicine, Cairo University. They were kept under standard environmental conditions of 12/12 hrs light/dark cycle, 25ºC, 55±5% humidity. Dogs were given regular dry food twice a day and unrestricted access to tap water during the study. They were acclimatized two weeks before the beginning of the experiment. Additionally, complete clinical examination, hematological evaluation, liver and kidney function tests were performed on each dog prior to ZnO NPs injections to exclude evidence of systemic diseases.

The block randomization method was used to allocate dogs into three groups ($n=3$, the experimental unit is a single animal). All dogs were subcutaneously injected by 3mL normal saline or ZnO NPs at different concentrations every day for one week in a circular manner at one side of the chest region. Group I received normal saline and kept as a control group, group II received 50 ppm ZnO NPs corresponding to 8 µg/kg bwt, and group III received 100 ppm ZnO NPs corresponding to 16 µg/kg bwt. To minimize the impact of potential confounders in our study, several strategies were implemented. First, the order of treatments and measurements were randomized to mitigate any bias introduced by the sequence of drug interventions. Furthermore, several steps were taken to control the potential influence of animal/cage location. The cages were arranged to minimize spatial effects, and the animals were rotated between cage locations throughout the study period. The personnel responsible for administering the treatments, conducting the measurements, and performing the assessments were blinded to the group assignments. While processing and analyzing the data, the experimenters were kept blind to the treatment. Because there isn't a reference dose of ZnO NPs in dogs, the doses were chosen based on the previous studies in mice that used ZnO NPs at low concentrations 250–500 ppm (50–100 µg/kg bwt) [27, 28], following the dose conversion formula between different species as the following:

Dog equivalent dose (mg/kg) = dose to be converted / (dog K_m/Mouse K_m
Whereas Dog K_m= 3, Mouse K_m=20

Each dog was admitted to routine physical examination, including general body condition (hair, skin, and body weight), appetite and mucus membrane. The experimental study would be stopped if there is a progressive weight loss (more than 20%), severe colic, unavoidable pain or distress, ulcerative dermatitis, echzyma, and other skin lesions. Since there were no reports of serious adverse events during the trial, all dogs were included in the study and none were excluded.

Radiographical and ultrasonographical examination

Radiographical examinations of the chest and abdomen were applied by left lateral recumbency of the dogs at the end of the experiment (7th day). Radiographs were independently blindly reviewed by three veterinary radiologists. Ultrasonographical examinations of the kidney, liver and spleen were applied at 7th day post-injection.

Sample collection

Fresh whole blood samples were collected from the right cephalic vein from all dogs at 0 day and 7th day after ZnO-NPs exposure. Some of them used immediately for hematological parameters, while others collected on anticoagulant and centrifuged at 3500 x.g for 5 min to isolate serum samples. Serum samples were preserved at -20°c till used for biochemical parameters. At the end of the experiment (7 days), all dogs were sedated with xylazine and butorphanol and then humanly euthanized using overdose of pentobarbital sodium (25 mg/kg bwt, intravenous injection through cephalic vein). Afterwards, skin at the site of injection and some organs (liver, kidneys, lungs, spleen, heart) were collected from all groups. Some samples were preserved at -80°c till used for oxidative stress evaluation and molecular studies, while others were fixed in 10% neutral buffer formalin till used for histopathological analysis.

Hematological and biochemical parameters

Fresh whole blood samples were used for hematological analysis (RBCs count, HB, PCV, MCV, MCHC, WBC count, differential leucocytic count using Giemsa stain, and Platelets counts) as previously described [29, 30].

Serum samples were used for estimating different biochemical parameters (AST, ALT, ALP, total proteins, albumin, urea, and creatinine) using highly specialized kits from Spectrum, Germany.

Oxidant/antioxidant assay

The collected frozen tissue samples (liver, kidney, and lung) were homogenized using ice-cold buffer (phosphate buffer saline, pH 7.4). Tissue homogenits were used to estimate malondialdehyde (MDA), and reduced glutathione (GSH) levels following the instruction of manufacturer's instructions of the standardized kits purchased from Biodiagnostic Co. Egypt.

Determination of the transcript levels of TNF-α, VEGF and IL-10 genes

The ABT Total RNA Mini Extraction Kit (Applied Biotechnology Co. Ltd, Egypt) was used to extract total RNA. Nanodrop Technology was utilized to assess the quantity and quality of RNA [31]. The ABT H-minus cDNA synthesis kit (Applied Biotechnology Co. Ltd, Egypt) was applied to create the cDNA. Following the manufacturer's instructions, ABT 2X SYBR mix (Applied Biotechnology co. ltd, Egypt) was used for the quantitative evaluation of cDNA amplification. The internal control was the GAPDH gene. The qRT-PCR primers are displayed in Table 1 and were created using the primer designing tool (Primer Designing Tool, n.d.). Triplicates of each qRT-PCR were run. The comparative $2^{-\Delta\Delta CT}$ approach was utilized to ascertain the relative transcription levels [32].

Histopathology

After 48 h from formalin fixation, all samples were washed and treated by the traditional method using ascending grade of alcohol for dehydration and xylene for clearance. After that, they embedded in paraffin wax to create blocks that an ordinary microtome could slice into 4.5 µm tissue sections. Hematoxylin and eosin stain (H&E) was used to color all sections, which were then examined under an Olympus BX43 light microscope. The DP27 Olympus camera, which was connected to Cell Sens dimensions software, took the pictures [33].

The ordinal Semiquantitative microscopic scoring system was performed to determine the extent of the pathological alterations in all the examined organs following the scheme described by Hassanen et al. [34], . The criteria used for grading the hepatorenal lesions were cellular degeneration, necrosis, vascular congestion, edema, hemorrhage, and interstitial inflammatory cells infiltration. Furthermore, the same parameters were graded distinctively in each pulmonary area, including bronchi, bronchioles, alveoli, and interstitial tissue to identify the histological distribution of lesions within the lung lobule according to Hassanen et al. [35], , whereas the spleen was graded via assessing the extent of lymphocytolysis [36]. The above-mentioned lesions were scored as mild, moderate, severe, and extensive severe, on a five-pointed ordinal scale, as following; 0=ordinal histology, 1<25%, 2=25:50%, 3=50:75%, and 4>75% tissue damage. All parameters were assessed by a pathologist who was not aware of the treatment groups to prevent bias.

Immunohistochemistry

The dewaxed-tissue sections were washed and blocked by peroxidase blocker (Sakura BIO), then the antigen retrieval was done by heat and citrate solution. After that, the primary antibody (Abcam, Ltd.) was added at a dilution of 1/200. Then, the materials involved in the immunostaining/DAB kit (Power-Stain 1.0 Poly HRP DAB Kit; Sakura) were added. The slides were counterstained with Haematoxylin, and finally inspected under a light microscope (Olympus BX43). Photomicrographs were taken using an Olympus DP27 digital camera connected to the Cell Sens dimensions program.

Statistical analysis

The data obtained from the present study were statistically subjected to one-way (ANOVA) and repeated measure ANOVA by the computerized program SPSS software, version "25" Data was represented as Mean±SD. Furthermore, the nonparametric values were analyzed using Kruskal Wallis H test and the Mann-Whitney U test, then the data was represented as the median. Values were considered significant at $P \leq 0.05$.

Results

Characterization of the prepared nanoparticles

Figure 1A displayed the X-ray diffraction patterns of ZnO NPs. The peaks at 2=31.77°, 34.42°, 36.25°, 47.54°, 56.59°, 62.85° and 67.95° were attributed to (100), (002), (101), (102), (110), (103), and (112) of ZnO NPs, indicating the crystalline structure of synthesized ZnO NPs that presented a hexagonal phase structure of the zincite mineral name (JCPDS 04-007-5097). HR-TEM images as illustrated in Fig. 1B demonstrated spherical-shaped particles with an average size of 19.3 nm.

Physical examinations

At the start point of the experiment (0 day), all dogs showed healthy body condition with normal value of temperature, heart rate, respiratory rate and capillary

Table 1 Primers sequences used for qRT-PCR

Gene symbol	Gene description	Accession number	Primer Sequence
TNF-α	Tumor necrosis factor	NM_001003244.4	F: 5′- CTCTCTGCCATCAAGAGCCC -3′ R: 5′- CTAAGCCTGAAGGGGGTGAG -3′
IL-10	Interleukin 10	NM_001003077.1	F: 5′- CGCTGTCACCGATTTCTTCC – 3′ R: 5′- GGTCGGCTCTCCTACATCTC – 3′
VEGFA	Vascular endothelial growth factor	*NM_001003175.2*	F: 5′-CCCGGTATAAACCCTGGAGC-3′ R: 5′-ACGCGAGTCTGTGTTTTTGC-3′
GAPDH	Glyceraldehyde3-phosphate dehydrogenase	NM_001003142.2	F: 5′- CGGGAAACTTGTCATCAACGG – 3′ R: 5′- TTTGGCTAGAGGAGCCAAGC – 3′

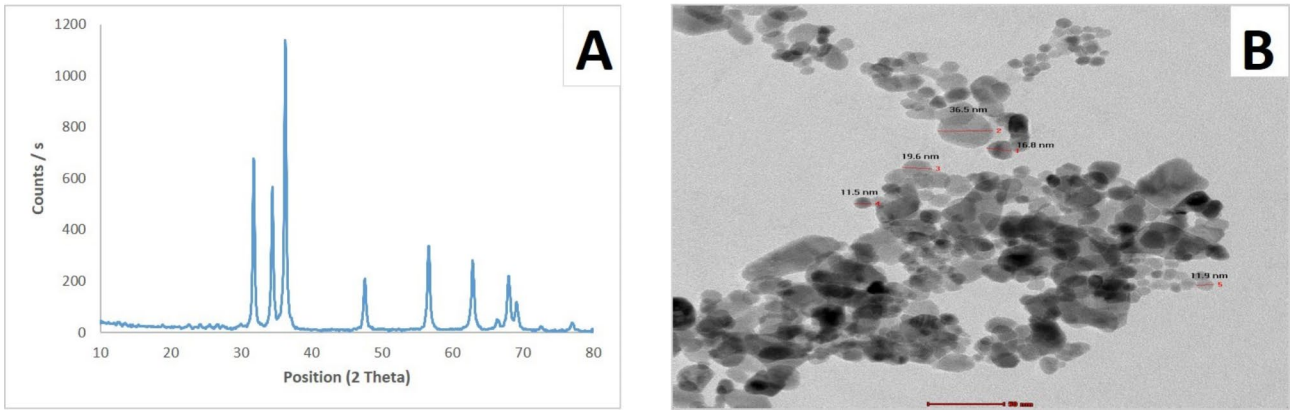

Fig. 1 Characterization of ZnO NPs. (**A**): XRD pattern analysis indicating the formation of ZnO NPs. (**B**): HR-TEM image showing nearly spherical shape of prepared ZnO NPs with average size 19.3 nm

refilling time. At 4 d post-injection till 7 d, the mucous membrane of dogs in the control group was rosy-red, whereas pale mucosa was observed in both 50 and 100 ppm receiving groups. The general body condition (appetite, hair, and body weight) had no evidence to be affected by ZnO NPs injections compared with the control group. Temperature, heart rate, respiratory rate and capillary refilling time in all groups are shown in Table 2. The temperature was constant in all treatment groups throughout the experiment. Whereas, both heart rates, respiratory rates, and capillary refilling time were significantly increased in the group receiving 100 ppm ZnO NPs compared with other groups. The cardiac sound of dogs in the control group and those receiving 50 ppm ZnO NPs was lup - dup sound through the period of the experiment while this sound was reduced from day 4 in group receiving 100 ppm and the sound disappeared at 7 d post-injection. Normal bronchial and vesicular sounds were heard in both the control group and 50 ppm ZnO NPs receiving group all over the experiment, however, a crackling sound was heard in the group receiving 100 ppm.

Radiological and ultrasonographic examinations

No obvious radiological changes in thoracic radiograph in the control group, while mild to moderate degree of pleural effusion manifested by thin radio dense line accumulated between the caudal and accessory lobes of the lungs was noticed in group receiving either 50 or 100 ppm ZnO NPs. Additionally, both ZnO NPs receiving groups showed a vascular pattern of pneumonia in which the pulmonary vessels became more visible as it engorged with blood along with a change of size, form, and direction. Moreover, a severe bronchial pattern of pneumonia which appeared as a ring-like shadow with tramline-like appearance was observed in the group receiving 100 ppm ZnO NPs. On the other hand, there were no obvious radiological changes observed in the abdominal radiography of both ZnO NPs receiving groups compared with the control group (Fig. 2)

The abdominal ultrasonographic examination of dogs in the control group showed normal homogenous parenchymal echogenicity of the liver with smooth capsule and regular contour. Moreover, the spleen had a uniform echotexture appearance of the head, body and tail and appeared slightly more hyperechoic than the liver. Additionally, the kidney appeared bean-shaped with smooth well-defined contour, and a thin linear hyperechoic renal capsule. On the other side, the abdominal ultrasonography of both ZnO NPs receiving groups showed moderate to marked alteration in the liver, spleen, and kidneys. The liver appeared heterogenous with parenchymal echogenicity and, thick and irregular capsule. The spleen also appeared heterogenous and slightly more hypoechoic than the liver besides the echotexture appearance of the head, body, and tail. The kidney had an ill-defined irregular contour with a thick hyperechoic renal capsule (Fig. 3).

Hematological and biochemical parameters

Hematological parameters that were presented in Table 3 revealed normal hematological profile in all groups at the start point of the experiment. At 7th day post-dosing, a significant decrease of HB, PVC, RBCS, and platelets count was recorded in ZnO NPs groups in a dose-dependent manner when compared to the control group. There was no significant difference in the level of MCV and MCHC between groups. Leukogram results showed a significant elevation of leukocytes and granulocytes as well as significant lymphocyte % reduction on the 7th day of ZnO NPs injection in a dose-dependent manner when compared to those of the control group.

There was not any significant difference in both liver and kidney function biomarkers across all experimental groups at the start point of the experiment. Moreover, a significant elevation of serum liver enzymes (AST, ALT,

Table 2 Mean value of Temperature, heart rate, respiratory rate, and capillary refilling time of various experimental groups at 0 day and after ZnO NPs exposure through 7 days

Days	Control	50 ppm	100 ppm
Temperature (ºc)			
0	37.5 ± 0.2 $^{a, A}$	37.4 ± 0.1 $^{a, A}$	37.5 ± 0.3 $^{a, A}$
1	37.6 ± 0.1 $^{a, A}$	38 ± 0.1 $^{b, B}$	37.9 ± 0.1 $^{b, A}$
2	37.8 ± 0.1 $^{a, A}$	38.1 ± 0.1 $^{b, B}$	38.4 ± 0.1 $^{c, B}$
3	38.2 ± 0.3 $^{a, B}$	38.1 ± 0.1 $^{a, B}$	38.4 ± 0.1 $^{a, B}$
4	38.1 ± 0.1 $^{a, B}$	38.2 ± 0.1 $^{a, B}$	38.5 ± 0.1 $^{b, B}$
5	38.1 ± 0.1 $^{a, B}$	38 ± 0.1 $^{a, B}$	38.4 ± 0.1 $^{a, B}$
6	38 ± 0.1 $^{a, A}$	38.1 ± 0.1 $^{a, B}$	38.4 ± 0.2 $^{b, B}$
7	38.2 ± 0.2 $^{a, B}$	38.1 ± 0.1 $^{a, B}$	38.5 ± 0.2 $^{a, B}$
Heart rate (bpm)			
0	76 ± 2.5 $^{a, A}$	76 ± 0.5 $^{a, A}$	75 ± 3.5 $^{a, A}$
1	76 ± 0.6 $^{a, A}$	75.3 ± 0.6 $^{a, A}$	74.7 ± 0.6 $^{a, A}$
2	75.3 ± 0.6 $^{a, A}$	76.3 ± 1.2 $^{a, A}$	89 ± 3.6 $^{b, B}$
3	76 ± 1 $^{a, A}$	79.7 ± 0.6 $^{b, B}$	117.3 ± 2.5 $^{c, C}$
4	76 ± 1 $^{a, A}$	81.7 ± 0.6 $^{b, B}$	131.7 ± 2.9 $^{c, D}$
5	77.3 ± 1.5 $^{a, B}$	80.1 ± 1.2 $^{a, B}$	153.3 ± 2.9 $^{b, E}$
6	76 ± 1 $^{a, A}$	80.3 ± 0.6 $^{b, B}$	158 ± 3.5 $^{c, E}$
7	79 ± 1 $^{a, C}$	81.1 ± 1.2 $^{a, B}$	167 ± 5.8 $^{b, F}$
Respiratory rate (bpm)			
0	15 ± 1.5 $^{a, A}$	15 ± 0.1 $^{a, A}$	15 ± 1.8 $^{a, A}$
1	15 ± 1 $^{a, A}$	14.7 ± 0.6 $^{a, A}$	15.3 ± 0.6 $^{a, A}$
2	17.7 ± 0.6 $^{a, B}$	19.7 ± 0.6 $^{b, B}$	19.7 ± 0.6 $^{b, B}$
3	19.3 ± 1.2 $^{a, C}$	21.7 ± 0.6 $^{b, C}$	29.7 ± 0.6 $^{c, C}$
4	19.7 ± 0.6 $^{a, C}$	25.3 ± 0.6 $^{b, D}$	39.3 ± 1.2 $^{c, D}$
5	20.1 ± 0.6 $^{a, D}$	25.6 ± 0.6 $^{b, D}$	44.7 ± 0.6 $^{c, E}$
6	21.3 ± 1.2 $^{a, D}$	29.3 ± 1.2 $^{b, E}$	47.3 ± 1.2 $^{c, F}$
7	21.7 ± 0.6 $^{a, D}$	30.1 ± 1.2 $^{b, E}$	49.3 ± 1.2 $^{c, F}$
Capillary refilling time (seconds)			
0	1.5 ± 0.1 $^{a, A}$	1.5 ± 0.1 $^{a, A}$	1.5 ± 0.1 $^{a, A}$
1	1.5 ± 0.1 $^{a, A}$	1.5 ± 0.1 $^{a, A}$	1.5 ± 0.1 $^{a, A}$
2	1.5 ± 0.1 $^{a, A}$	1.5 ± 0.1 $^{a, A}$	1.5 ± 0.1 $^{a, A}$
3	1.5 ± 0.1 $^{a, A}$	1.7 ± 0.1 $^{a, b, B}$	1.8 ± 0.2 $^{b, B}$
4	1.5 ± 0.1 $^{a, A}$	1.7 ± 0.1 $^{b, B}$	2.1 ± 0.1 $^{c, C}$
5	1.5 ± 0.1 $^{a, A}$	1.7 ± 0.1 $^{a, B}$	2.8 ± 0.3 $^{b, D}$
6	1.5 ± 0.1 $^{a, A}$	1.9 ± 0.1 $^{b, C}$	3.2 ± 0.2 $^{c, E}$
7	1.5 ± 0.1 $^{a, A}$	2 ± 0.1 $^{b, D}$	3.4 ± 0.2 $^{c, F}$

Values presented as mean ± SD (n = 3). Small letters (a, b, c) mean significant difference between groups at $P \leq 0.05$, while capital letters (A, B, C, D, E, F) mean significant difference between time points (1-7th day postdosing) at $P \leq 0.05$. Notes: normal temperature in dogs: 37-38.8ˊc, heart rates: 80–160 bpm, respiratory rates: 15–30 bpm, capillary refilling time: < 2 s

and ALP) and kidney function parameters (urea and creatinine) were recorded after 7 days of ZnO NPs in a dose-dependent manner when compared to the control group. Furthermore, the group received 100 ppm showed a significant reduction of total proteins and albumin after 7 days of ZnO NPs exposure (Table 4).

Oxidant/antioxidant assay

Data presented in Table 5 revealed a significant elevation of hepatic, renal and pulmonary MDA levels in a dose-dependent manner in diverse groups, while liver, kidney, and lung GSH were significantly reduced in both ZnO NPs receiving groups compared with the control group.

The transcript levels of TNF-α, VEGF and IL-10 genes

ZnO NPs induced a significant upregulation of the hepatic, renal, and pulmonary transcript levels of pro-inflammatory cytokine TNF-α and VEGFA compared with the control group. Whereas the anti-inflammatory marker IL-10 showed downregulation in all the examined organs of ZnO NPs groups in a dose-dependent manner (Fig. 4).

Histopathology

Liver, kidneys, and spleen tissue sections obtained from dogs in the control group didn't exhibit any histological alterations (Fig. 5a-c). Otherwise, the 50 ppm ZnO NPs receiving group demonstrated abnormalities in the histological structure of some organs. The liver showed moderate random hepatocellular vacuolar degeneration with sporadic cell necrosis (Fig. 5d). Kidney sections showed mild to moderate tubular epithelial degeneration with sparse glomerular degeneration (Fig. 5e). The spleen noticed mild lymphoid depletion in some follicles (Fig. 5f). Meanwhile, the group receiving 100 ppm ZnO NPs displayed substantial histopathological changes in every area that was examined. Sections of the liver observed hepatocellular degeneration and necrosis along with sinusoidal congestion and lymphocytic exocytosis (Fig. 5g1). The hepatic parenchyma was covered through diffuse to coalescing areas of hemorrhage (Fig. 5g2). Kidney tissues noticed severe degenerative and necrobiotic conditions in the epithelium of renal tubules (Fig. 5h1). The interstitial tissue showed multifocal to coalescing inflammatory cells infiltration (Fig. 5h2). The splenic section showed severe lymphocytolysis in most white pulp (Fig. 5i1-i2).

Regarding heart, skin, and lung tissue sections, we didn't notice any histological changes in the control group (Fig. 6a-c) Likewise, both heart and skin tissues showed normal histological organization in 50 ppm receiving group (Fig. 6d, e). The lung sections showed severe bronchitis and bronchiolitis manifested by degeneration and necrosis of its epithelial lining and a high number of inflammatory cells infiltrated in both mucosal and submucosal layers (Fig. 6f1). There was alveolar damage with intra-alveolar edema, hemorrhage, and inflammatory cell infiltration (Fig. 6f2). On the other hand, the group receiving 100 ppm ZnO NPs demonstrated moderate myocardial degeneration and necrosis along with few inflammatory cell infiltrations. Extensive thickening of the pericardial layer by edema was observed in most sections (Fig. 6g). The skin tissue sections showed mild

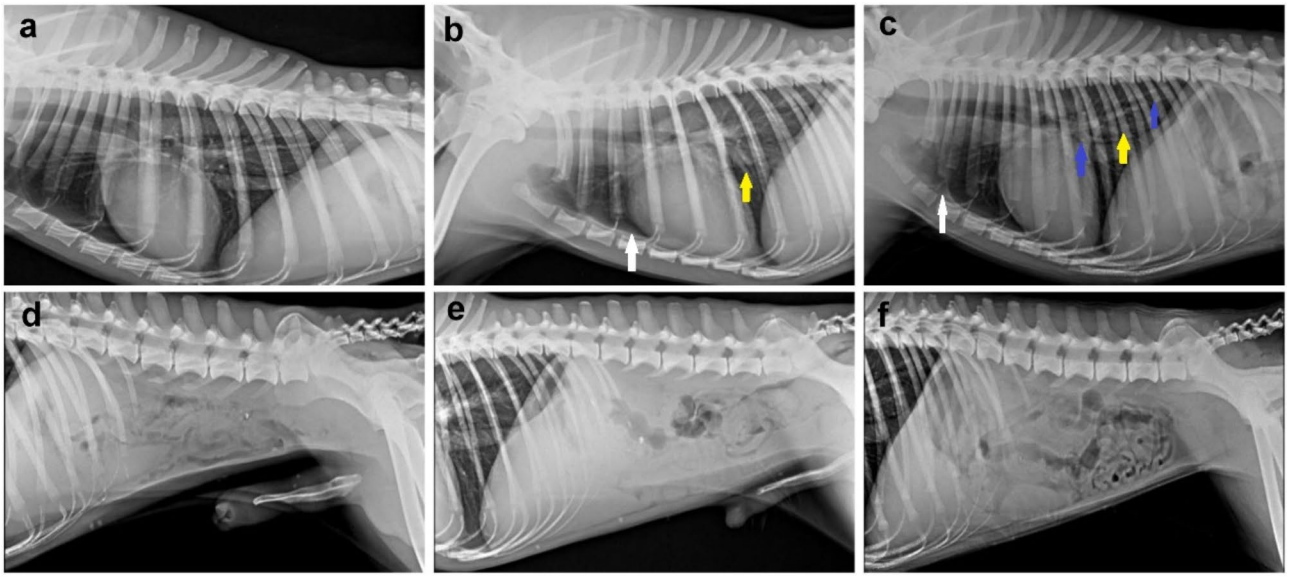

Fig. 2 Radiographic examination of dogs in various groups. (**a**-**c**) Left lateral thoracic radiograph representing, (**a**) control group has normal lung and cardiac silhouette. (b & **c**) groups receiving 50 and 100 mg ZnO NPs, respectively, showed mild to moderate radiographic changes. Note: pleural effusion (white arrow), vascular pattern of pneumonia (yellow arrow), bronchial pattern of pneumonia (blue arrow). (**d**-**f**) Normal abdominal radiograph of all ZnO NPs receiving groups

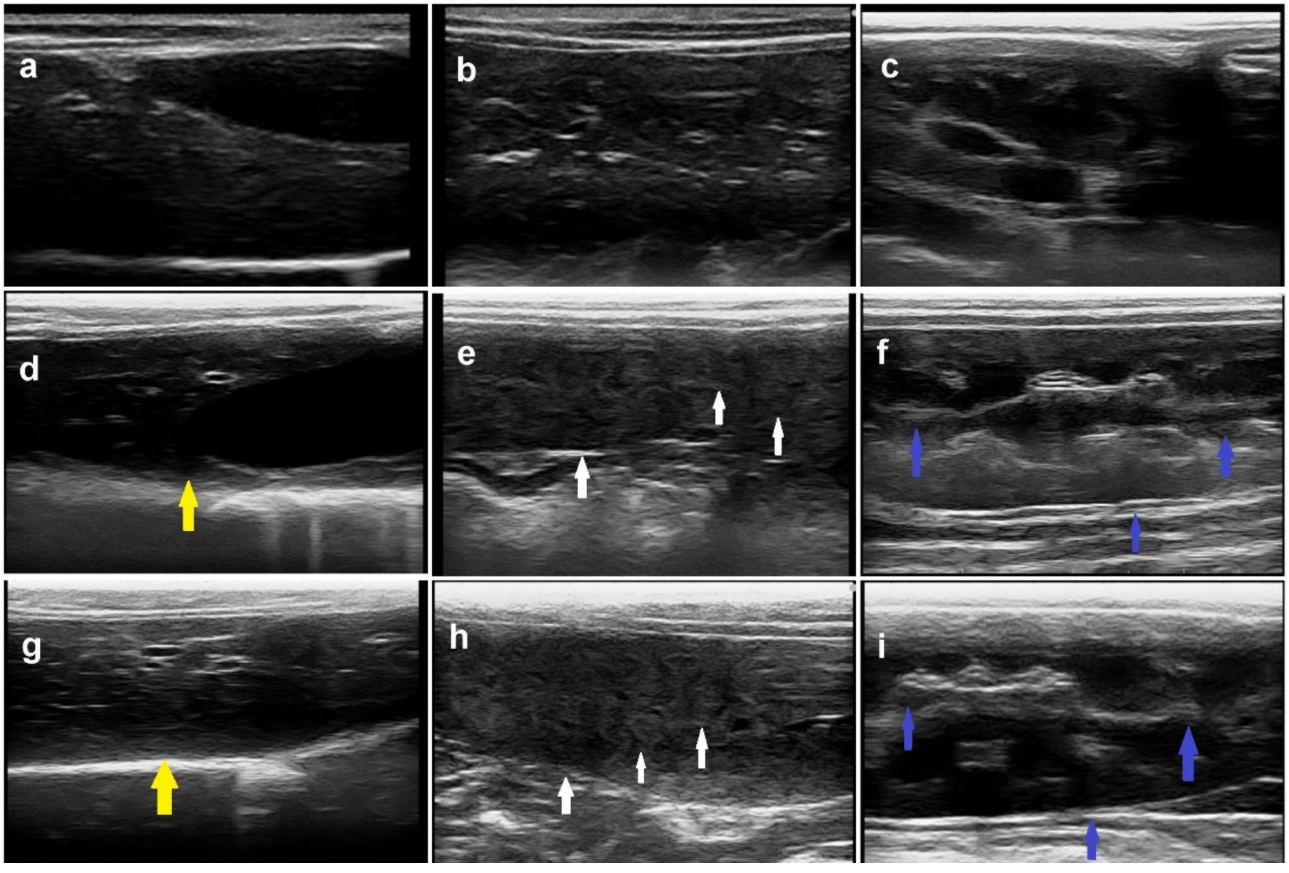

Fig. 3 Abdominal ultrasonography of dogs in various groups. (**a**-**c**) Dog in the control group showed normal appearance of liver, spleen, and kidneys. (**d**-**f**) Dog receiving 50 ppm ZnO NPs, and (**g**-**i**) dog receiving 100 ppm ZnO NPs displayed various changes in some organs. Note: heterogenous liver with parenchymal echogenicity and severe thick capsule (yellow arrow), heterogenous hypoechoic spleen with echotexture appearance of the head, body, and tail (white arrow), kidney with thick hyperechoic capsule and ill-defined parenchyma (blue arrow)

Table 3 Hematological parameters of various experimental groups at 0 day and 7 days after ZnO NPs exposure

Parameters /groups	Control	50 ppm	100 ppm
At 0 day			
HB (g/dl)	14.10 ± 0.50 [a]	14.16 ± 0.76 [a]	14.00 ± 0.55 [a]
HCT %	37.13 ± 0.41 [a]	37.00 ± 0.50 [a]	37.16 ± 0.37 [a]
RBCs ×10^6 cell/µl	6.13 ± 0.45 [a]	6.36 ± 0.66 [a]	6.08 ± 0.52 [a]
MCV (fL)	61.13 ± 5.10 [a]	58.27 ± 5.99 [a]	61.73 ± 5.50 [a]
MCHC (%)	37.95 ± 1.00 [a]	38.30 ± 2.19 [a]	37. 57 ± 1.21 [a]
WBCs ×10^3 cell/µl	10.66 ± 1.26 [a]	11.13 ± 1.40 [a]	11 0.22 ± 1.48 [a]
Granulocytes (%)	70.33 ± 4,72[a]	72.33 ± 4.73 [a]	71.66 ± 5.50 [a]
Lymphocytes (%)	27.33 ± 4.93 [a]	25. ± 5.56 [a]	24.33 ± 1.00 [a]
Monocytes (%)	2.33 ± 0.58 [a]	2.66 ± 1.15 [a]	4.00 ± 1.00 [a]
Platelets ×10^3cell/µl	206.33 ± 24.70 [a]	209.67 ± 17.04 [a]	208 ± 23.30 [a]
At 7 days			
HB(g/dl)	13.53 ± 0.50 [a]	12.77 ± 0.50 [a, b]	12.33 ± 0.28 [b]
HCT (%)	36.56 ± 0.40 [a]	35.97 ± 0.45 [a, b]	35.53 ± 0.39 [b]
RBCs ×10^6 cell/µl	5.81 ± 0.45 [a]	4.97 ± 0.41 [a, b]	4.78 ± 0.41 [b]
MCV(f/l)	63.09 ± 4.52 [a]	72.73 ± 6.60 [a]	74.62 ± 5.74 [a]
MCHC (%)	37.00 ± 1.00 [a]	35.50 ± 1.51 [a]	34.71 ± 1.02 [a]
WBCs ×103 cell/µl	11.80 ± 1.35 [a]	16.49 ± 1.10 [b]	17.57 ± 1.30 [b]
Granulocytes (%)	72.33 ± 4.62 [a]	80.00 ± 4.36 [a, b]	85.00 ± 4.00 [b]
Lymphocytes (%)	25.33 ± 5.78 [a]	17.66 ± 4.73 [a, b]	12.33 ± 4.04 [b]
Monocytes (%)	2.33 ± 1.15 [a]	2.33 ± 0.58 [a]	2.66 ± 0.58 [a]
Platelets ×10^3cell/µl	205.33 ± 22.48 [a]	189.67 ± 17.09 [a, b]	151.67 ± 16.07 [b]

Values presented as mean ± SD (n = 3). Small letters (a, b,c) mean significant difference between groups at $P \leq 0.05$. Abbreviations: HB: hemoglobin, HCT: hematocrit, RBCs: red blood corpuscles, MCV: mean corpuscular volume, MCHC: mean corpuscular hemoglobin concentration. MCV = HCT×10/RBCS

MCHC = HB×100/HCT

Table 4 Some biochemical parameters of various experimental groups at 0 day and 7 days after ZnO NPs exposure

Parameters /groups	Control	50 ppm	100 ppm
At 0 day			
AST (U/L)	38.50 ± 5.00 [a]	39.67 ± 5.51 [a]	38.68 ± 3.51 [a]
ALT(U/L)	52.68 ± 6.43 [a]	55.43 ± 6.67 [a]	52.50 ± 6.38 [a]
ALP (U/L)	53.83 ± 8.5 [a]	52.00 ± 8.00 [a]	56 ± 9.17 [a]
Total proteins (g/dl)	5.90 ± 0.85 [a]	6.33 ± 0.62 [a]	5.93 ± 0.95 [a]
Albumin (g/dl)	3.28 ± 0.85 [a]	3.79 ± 0.93 [a]	3.15 ± 1.00 [a]
Urea (mg/dl)	11.17 ± 1.60 [a]	12.74 ± 2.74 [a]	11 0.97 ± 1.76 [a]
Creatinine (mg/dl)	0.90 ± 0.05 [a]	0.96 ± 0.06 [a]	0.95 ± 10.06 [a]
At 7 day			
AST (U/L)	40.33 ± 5.03 [a]	64.33 ± 6.43 [b]	89.67 ± 9.50 [c]
ALT(U/L)	52.00 ± 5.29 [a]	100.43 ± 17.15 [b]	152.33 ± 27.65 [c]
ALP (U/L)	56.33 ± 7.64 [a]	86.33 ± 10.41 [a, b]	118.4 ± 23.63 [b]
Total proteins (g/dl)	5.83 ± 0.95 [a]	6.27 ± 0.93 [a]	4.93 ± 0.90 [b]
Albumin (g/dl)	3.16 ± 0.75 [a]	3.57 ± 0.84 [a]	2.37 ± 0.84 [b]
Urea (mg/dl)	10.87 ± 2.01 [a]	17.97 ± 2.59 [a, b]	21.87 ± 3.78 [b]
Creatinine (mg/dl)	1.13 ± 0.24 [a]	1.88 ± 0.39 [a, b]	2.38 ± 0.47 [b]

Values presented as mean ± SD (n = 3). Small letters (a, b, c) mean significant difference between groups at $P \leq 0.05$

Abbreviations: AST: aspartate aminotransferase, ALT: alanine amino transferase, ALP: alkaline phosphatase

Table 5 Effect of ZnO NPs on different oxidative stress parameters at 7th day

	Control	50 ppm	100 ppm
MDA level (nmol /g tissue)			
Liver	29.00 ± 3.60 [a]	48.33 ± 7.64 [b]	68.00 ± 9.85 [c]
Kidney	43.00 ± 9.85 [a]	69.00 ± 8.54 [b]	85.33 ± 11.02 [b]
Lungs	15.67 ± 4.04 [a]	31.33 ± 7.09 [a, b]	48.33 ± 7.64 [b]
GSH content (mg/g tissue)			
Liver	45.67 ± 10.69 [a]	41.267 ± 3.66 [b]	21.13 ± 3.44 [c]
Kidney	39.33 ± 5.13 [a]	21.57 ± 3.46 [b]	15.00 ± 3.00 [b]
Lungs	34.67 ± 4.50925 [a]	17.67 ± 2.52 [b]	12.23 ± 1.26 [b]

Values presented as mean ± SD (n = 3). Small letters (a, b, c, d) mean significant difference between groups at $P \leq 0.05$. MDA: malondialdehyde, GSH: reduced glutathione

dermal edema and inflammatory cell infiltration (Fig. 6h). The group receiving 100 ppm ZnO NPs displayed extensive bronchitis and bronchiolitis with extensive alveolar damage and diffuse hemorrhage (Fig. 6i1). Most blood vessels showed vasculitis manifested by intimal and medial degeneration with vascular and perivascular inflammatory cell infiltration (Fig. 6i2).

The scoring scheme of all examined organs was summarized in Table 6. The heist scores were recorded in the group receiving 100 ppm ZnO NPs followed by those receiving 50 ppm.

Immunohistochemistry

Liver, kidneys, and lung sections of the control group showed negative to normal baseline caspase-3 protein expression. Otherwise, those obtained from both 50 and 100 ppm ZnO NPs receiving group displayed a

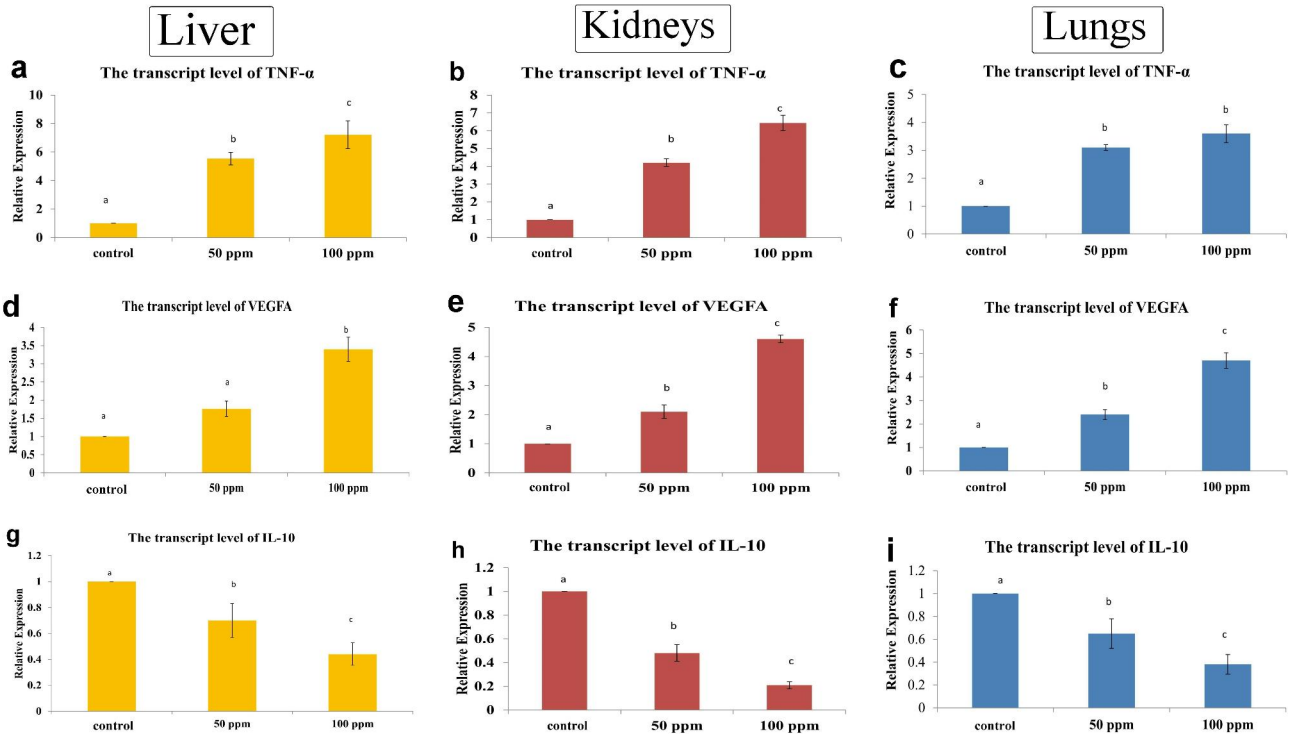

Fig. 4 Bar charts representing the transcriptase level of some genes in the liver, kidneys, and lungs of dogs in various groups. (**a**-**c**) TNF-α, (**d**-**f**) VEGF, and (**g**-**i**) IL-10. Values presented as mean ± SD ($n = 3$). Various letters (**a**, **b**, **c**) mean significant difference between groups at $P \leq 0.05$

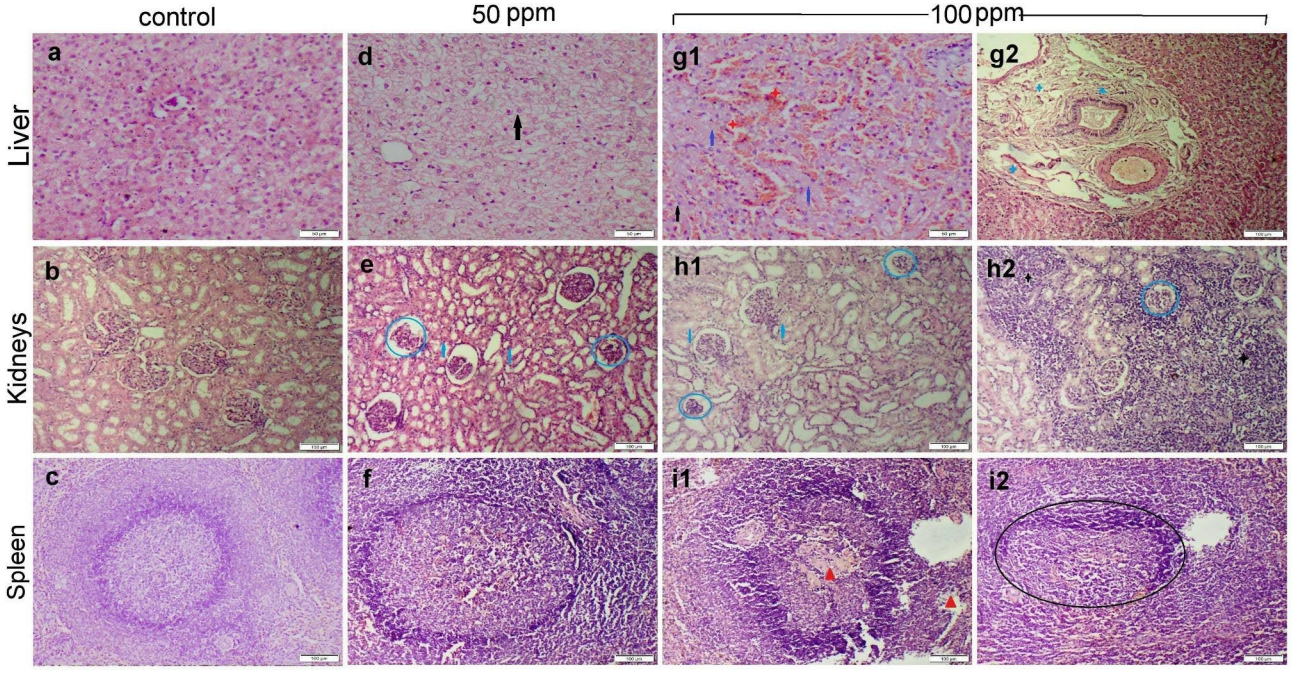

Fig. 5 Photomicrographs representing various organ sections stained by H&E obtained from different experimental groups. (**a**-**c**) Liver, kidney, and spleen sections, respectively, obtained from the control group showed normal histology. (**d**-**f**) Liver, kidneys, and spleen sections, respectively, obtained from group receiving 50 mg ZnO NPs showed mild histological changes. (**g**-**i**) Liver, kidneys, and spleen sections, respectively, obtained from group receiving 100 mg ZnO NPs showed severe histopathological alterations. Note: cellular degeneration (black arrow), necrosis (blue arrow), glomerular damage (blue circle), hemorrhage (red star), edema (blue star), fibrosis (blue triangle), inflammatory cells (black star), lymphoid depletion (red triangle), incomplete ill-defined follicle (black circle)

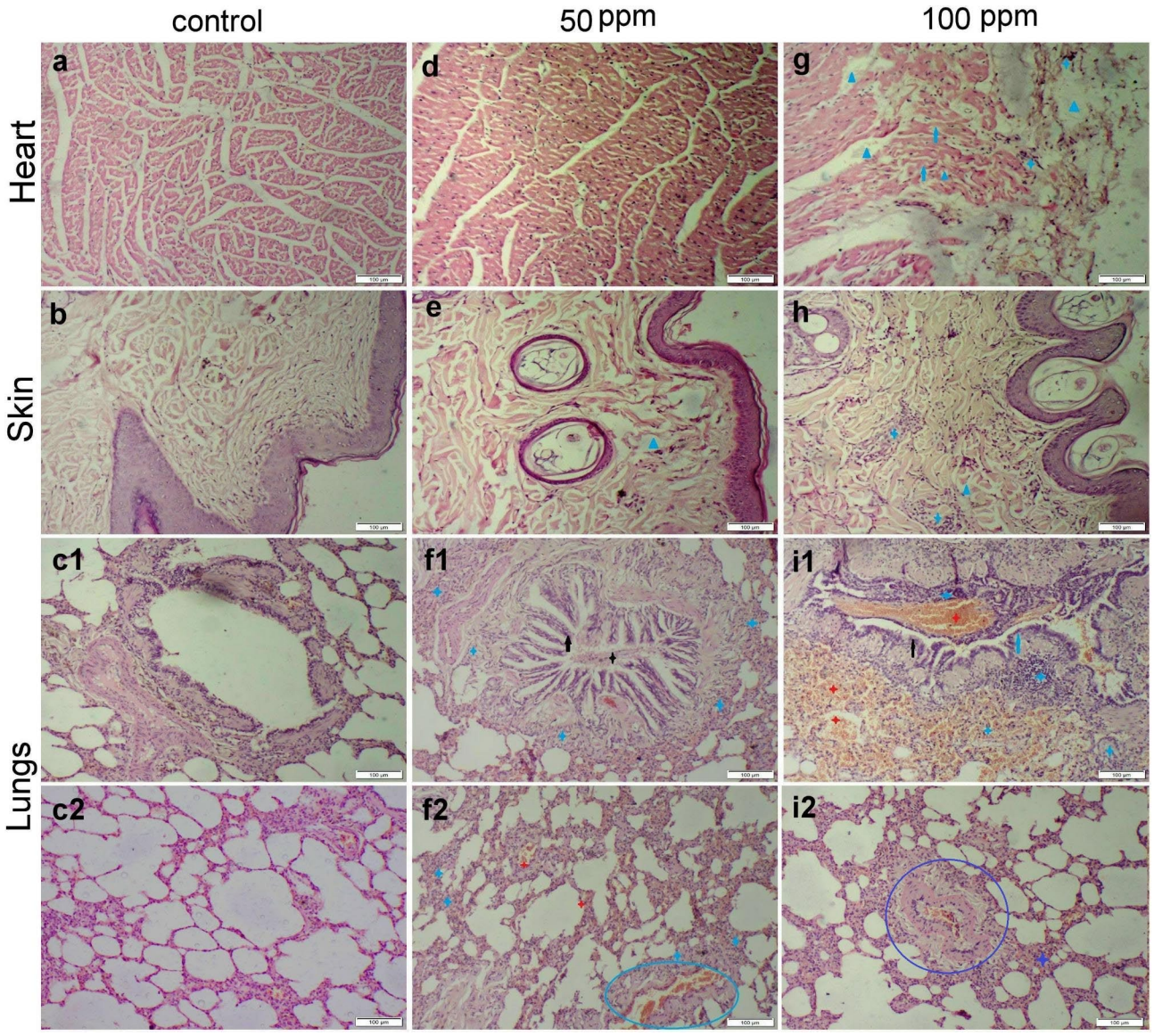

Fig. 6 Photomicrographs representing various organ sections stained by H&E obtained from different experimental groups. (**a**-**c**) Heart, skin, and lung sections, respectively, obtained from the control group showed normal histology. (**d**-**f**) Heart, skin, and lung sections, respectively, obtained from group receiving 50 mg ZnO NPs showed normal histological structure of both myocardium and skin tissue along with moderate histological changes in the pulmonary tissues. (**g**-**i**) Heart, skin, and lung sections, respectively, obtained from group receiving 100 mg ZnO NPs showed severe histopathological alterations. Note: epithelial hyperplasia (black arrow), necrosis (blue arrow), intraluminal exudates (black star), inflammatory cells (blue star), vasculitis (blue circle), hemorrhage (red star), edema (blue triangle)

dose-dependent increase in casp-3 immunopositivity whereas, the strongest expression was noticed in the 100 ppm receiving group. In general, casp-3 expression in the lungs was higher than other organs followed by kidneys and liver finally (Fig. 7).

Discussion

Nanotechnology has been extensively applied in all fields of veterinary medicine and animal science [37]. Recently, ZnO NPs have gained interest owing to their potential antimicrobial, antitumorigenic, wound remodeling, UV scattering, and angiogenic properties [38, 39]. In the current study, ZnO NPs induced dose and time-dependent increase in temperature, heart rate, respiratory rate and capillary refilling time indicate poor health condition of dogs. Physical examinations are the most important and challenging practical skills that provide valuable expectations about dogs' health and general body condition [40]. The pale mucosa of dogs receiving 100 ppm proved the incidence of anemia in this group [41]. A significant elevation of heart and respiratory rates in dogs receiving 100 ppm ZnO NPs suggested the cardiopulmonary toxicity

Table 6 The microscopic lesion scoring of the examined organs of different experimental groups

	Control	50 ppm	100 ppm
Hepatic lesion scoring			
Hepatocellular degeneration	0 [a]	2 [b]	3 [c]
Hepatocellular necrosis	0 [a]	3 [b]	4 [c]
Hemorrhage	0 [a]	0 [a]	3 [b]
Portal edema	0 [a]	1 [b]	4 [c]
Portal inflammation	0 [a]	1 [b]	2 [c]
Renal lesion scoring			
Tubular degeneration	0 [a]	2 [b]	3 [c]
Tubular necrosis	0 [a]	2 [b]	3 [c]
Glomerular damage	0 [a]	2 [b]	3 [c]
Interstitial inflammation	0 [a]	1 [b]	4 [c]
Interstitial hemorrhage	0 [a]	0 [a]	0 [a]
Pulmonary lesion scoring			
Bronchitis and bronchiolitis	0 [a]	2 [b]	4 [c]
Alveolar damage	0 [a]	1 [b]	4 [c]
Alveolar edema	0 [a]	1 [b]	3 [c]
Alveolar hemorrhage	0 [a]	0 [a]	4 [b]
Interstitial edema	0 [a]	0 [a]	3 [b]
Interstitial hemorrhage	0 [a]	1 [b]	4 [c]
Interstitial inflammation	0 [a]	2 [b]	4 [c]
Vasculitis	0 [a]	3 [b]	4 [c]
Splenic lesion scoring			
Lymphoid depletion	0 [a]	0 [a]	4 [b]
Cardiac lesion scoring			
Myocardial degeneration	0 [a]	1 [b]	2 [b]
Myocardial edema	0 [a]	0 [a]	2 [b]
Pericardial edema	0 [a]	0 [a]	4 [b]

Data expressed as median ($n=35$ microscopic fields/group). Small letters (a, b, c) mean significant difference between groups at $P \leq 0.05$

induced by ZnO NPs. Additionally, ZnO NPs-induced oxidative stress could activate the sympathetic nervous system resulting in an increase in temperature, heart, and respiratory rates [42]. Whereas an increase in capillary refilling time in this group reflects the abnormal perfusion to the peripheral tissues due to ZnO NPs-inducing cardiovascular lesions and anemia. Moreover, the systemic abnormalities induced by ZnO NPs injections were reflected in the radiological and ultrasonographic examinations of many organs, including lungs, liver, spleen, and kidneys. All these findings suggest the toxic effect of ZnO NPs on various organs of dogs.

In the present study, ZnO NPs induced dose-dependent increase in both liver and kidney function biomarkers, involving AST, ALT, ALP, BUN, and Creatinine. Furthermore, the total proteins and albumin levels were significantly decreased in the group receiving 100 ppm ZnO NPs compared to other groups. The liver plays a crucial role in metabolism, digestion, detoxification, and elimination of xenobiotic substances from the body [43]. ALT and AST are liver cytosolic and mitochondrial isoenzymes, and their serum activity is significantly elevated in case of hepatocellular damage [28, 44]. While the alkaline phosphatase enzyme, zinc metalloenzyme family, is strongly activated in microvilli within the bile canaliculus. Serum alkaline phosphatase is an important biomarker associated with bone, liver, and other diseases [45]. Additionally, serum total proteins and albumin levels decreased in patient with any liver disease [46]. Concerning, BUN and creatinine, they reflect the glomerular filtration rate (GFR) and renal dysfunction [47]. ZnO NPs could promote the lysosomal autophagy like other nanoparticles leading to cell damage [48]. The increased number of lysosomes in the epithelial lining the proximal convoluted tubule leading to organelles damage [49].

The elevated liver and kidney function biomarkers in both ZnO NPs receiving groups suggested remarkable hepatorenal toxicity induced by ZnO NPs which affects the membrane permeability of cells. The hepatotoxic effect of ZnO NPs has been formerly reported either in rodents [48, 50, 51], or in vitro [52]. Furthermore, its hepatotoxic and nephrotoxic potential has been previously elucidated in Nile tilapia through oxidative damage to these organs [53, 54]. Through oxidative stress, ZnO NPs caused renal damage in both vitro and vivo models [55]. These findings were consistent with the histopathological results that demonstrated extensive hepatocellular and tubular epithelial degeneration and necrosis in groups receiving 50 and 100 ppm ZnO NPs. Additionally, there was extensive cellular degeneration and necrosis along with widespread inflammation in other organs, including the lungs, heart, and spleen in relation to the dose of ZnO NPs. The size and concentration of ZnO NPs are the major factors that determine the histopathological alterations they cause [56]. It has been reported that nanoparticles toxicity varies among animal species and based on the NPs size, concentration, duration, and routes of exposure [57]. Nanoparticles can enter the body and rapidly reach circulation via several routes such as inhalation, dermal, oral, and injections [58]. Once the entrance of ZnO NPs into the circulation, it is rapidly distributed to various organs, particularly liver, spleen, lungs, kidneys, and heart [59–61]. Then it interact with several biological components releasing reactive oxygen species (ROS) and highly reactive free Zn ions that cause oxidative stress damage to target organs [20, 62]. ROS overgeneration causes cell and organelle membrane damage because of lipid peroxidation as well as mitochondrial dysfunction [21]. From another point, free Zn ions caused lysosomal disruption that induced the release of their contents into the cytosol leading to cell apoptosis and necrosis [22, 63]. ZnO NPs could bind with the protein which may contribute to their cytotoxicity [57]. Several studies showed hepatorenal damage in mice following oral exposure to ZnO NPs [56, 64–66]. Another study revealed that oral gavage

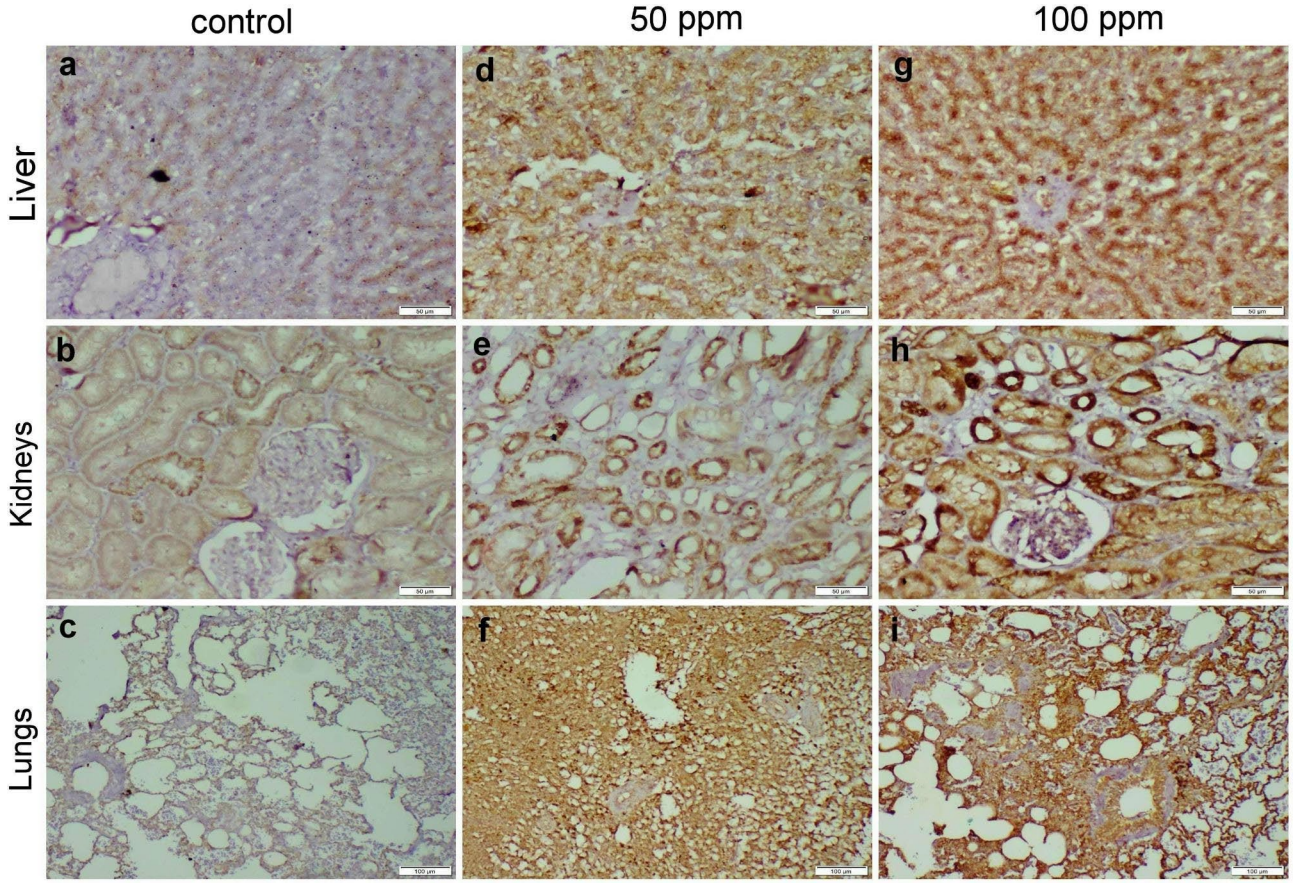

Fig. 7 Photomicrographs representing caspase-3 immunoexpression in different organs of ZnO NPs-exposed groups. (**a**-**c**) control group demonstrated negative casp-3 protein expression in the liver, kidneys, and lung tissues. (**d**-**f**) group receiving 50 mg ZnO NPs and (**g**-**i**) group receiving 100 mg ZnO NPs, both groups displayed strong casp-3 immunopositivity in all the examined organs

of rats with ZnONPs could induce hepatocellular necrosis with extensive sinusoidal congestion [50].

The findings of the current study revealed a significant elevation of MDA levels with depletion of GSH levels in hepatic, renal, and pulmonary tissues of ZnO NPs receiving groups. An in-vitro study proved that ZnO NPs caused oxidative DNA damage and ROS-triggered mitochondria-mediated death in human liver cells (HepG2) [67]. Another study showed that ZnO NPs led to oxidative stress-mediated hepatotoxicity in rats [68]. Exposure to ZnONPs induces lung oxidative stress and cellular damage in mice [69]. Furthermore, In vitro and in vivo studies show that ZnO NPs cause acute lung injury through oxidative stress-mediated mitochondrial damage and NLRP3 inflammasome activation [70]. Also, it show cytotoxicity and genotoxicity through oxidative stress responses in human lung fibroblasts [71]. On the other hand, ZnO NPs caused renal injury by triggering oxidative stress, mitochondrial damage, and apoptosis in renal tubular epithelial cells [72].

Oxidative stress-induced apoptosis, as well as induction of JNK/p38MAPK and STAT-3 signaling pathways, are likely to be responsible for ZnONPs-induced hepatotoxicity [50]. It has been recently reported that excessive exposure to ZnO NPs can cause an imbalance of the intestinal microbiome and hepatic metabolites in dogs, ultimately resulting in liver damage [73]. Oxidative stress induced by ZnO NPs resulted in kidney damage, accompanied by increased ROS and MDA levels and a decrease in SOD levels both in-vitro and in-vivo [55]. Furthermore, oxidative stress-induced apoptosis can be considered one of the pulmonary toxicity pathways induced by ZnO-NP exposure [74]. This comes in parallel with our findings that showed a significant elevation of pulmonary lipid peroxidative damage (MDA) and a decrease in lung GSH levels along with marked pulmonary pathological alterations in both ZnO NPs receiving groups. Previous study was noticed oxidative stress-mediated pulmonary inflammation and widespread alveolar damage in mice after intratracheal instillation of ZnONPs [27]. One study revealed that intraperitoneal injection of ZnONPs caused cellular degeneration and necrosis with inflammatory reactions in liver and lung tissue of mice [75]. Similar

findings recorded in other study but in the liver and heart tissue of mice [76].

So that, the vascular and bronchial patterns of pneumonia that have been noticed in the radiological examination of ZnO NPs groups could be explained by the alveolar and interstitial hemorrhage and inflammatory cells infiltration noticed via histopathological examination. The above-mentioned lesions resulted in marked thickening of the interalveolar septa which led to a narrowing of the bronchi and alveoli, so the bronchial pattern was developed in radiographs [77]. Additionally, the microscopic appearance of interstitial pulmonary congestion along with perivascular edema and hemorrhage could explain the pleural effusion that appeared in the radiographs of the 100 ppm ZnO NPs group. Regarding the ultrasonographic examination, the liver, spleen, and kidney of the 100 ppm ZnO NPs group appeared as heterogenous echogenicity with thickened capsules because of oxidative stress-mediated apoptosis and focal necrosis as previously explained. Additionally, the spleen became more hypoechoic than the liver because of ROS/Zn ions-induced hemorrhage [78].

Furthermore, ZnO NPs caused dose-dependent lymphocytolysis and lymphoid depletion of the splenic white pulp. ZnO NPs can induce immunotoxicity either indirectly via ROS generation or directly via invading the immune cells [25, 79]. In general, NPs are internalized by immune cells such as macrophages, lymphocytes, and dendritic cells, by either endocytosis or phagocytosis based on particle size [80]. Recent studies demonstrated a remarkable increase in Zn levels in the immune organs of mice involving liver, spleen, and thymus after 14 days of oral intake of ZnO NPs [81]. Following antigen presentations by B cells to T helper cells, this immunogenicity can mediate cytokine production and evoke cytotoxicity of the immune cells [82]. Upon hematological examination in the present study, HB, PCV, RBCs, and platelet count were significantly lowered between diverse groups in a dose-dependent manner, besides normal MCV and MCH indicating the incidence of normocytic normochromic anemia. This could be attributed to the shorter life span of erythrocytes due to elevated ROS production [83]. Equivalent results were obtained in various experimental studies of rodents and fish [84, 85]. Platlets reduction and hematotoxic effects of ZnO NPs have been previously reported in rats [51, 86]. This confirms that ZnO NPs were hematotoxic, especially in higher doses in Mongrel dogs. Moreover, the leukogram revealed a significant granulocytosis and lymphocytopenia. This feature may be the same as those following exposure to glucocorticoids in animals due to depletion of lymphocytes in lymphoid organs [87]. Whereas the granulocytosis is a marker of acute inflammatory response that induced by ZnO NPs as mentioned previously. It has been reported that ZnO NPs could induce inflammatory responses as the released Zn ions could activate specific pathways to produce chemokines to recruit granulocytes to the sites of ZnO NPs exposure [88].

In the present study, oxidative stress can play a pivotal role in ZnO NPs-induced toxicity in dogs. There are several pathological processes attributed to ZnO NPs-induced toxicity including apoptosis, necrosis, and inflammation. The liver, kidneys, and lungs of both ZnO NPs exposed groups displayed strong casp-3 protein expression which is consistent with earlier studies in mice [27, 89]. One study revealed that ZnONPs-mediated oxidative stress could induce testicular apoptosis via activation of Bax, caspase-3, and inhibition of Bcl-2 [90]. Another study using a murine macrophage cell line found that the caspase-3 upregulation is involved in ZnO-mediated apoptosis [91]. Oxidative stress can trigger apoptosis by opening the mitochondrial transition pores allowing the cytochrome c and Ca ions to release into the cytosol [92]. Cytochrome c initiates activation of the caspase cascade and subsequently leads to cell apoptosis [93]. Moreover, the cytosolic Ca ions activate several enzymes such as protease, phospholipase, protein kinase, and endonuclease leading to further cell injury and death [94]. From the molecular insights, both ZnO NPs exposed groups showed upregulation of the transcript levels of TNF-α and VEGF and downregulation of IL10 in liver, kidneys, and lungs indicating the inflammatory reactions and necrobiotic changes induced by ZnO NPs in such organs. A recent study revealed the ability of ZnO NPs to initiate acute inflammatory reactions in mouse lung via phagocytic activity and release of free Zn ions [88]. An in-vitro study showed that exposure to ZnO NPs could trigger oxidative stress, which in turn activate the pro-inflammatory cytokines [95]. Another study found that TNF-α and IL-6 were elevated in the blood of ZnO NPs exposed rats [96]. Additionally, the overexpression of VEGFA induced vasodilation and extensive infiltration of macrophages and granulocytes to ZnO NPs-exposed area resulting in acute inflammatory reactions in target organs leading to further oxidative stress [97].

Although the present study is intensive and included important findings regarding ZnO NPs toxicity in dogs, it also had some limitations including, a lack of measuring residual levels of zinc ions in various organs, lack of measuring more immunological parameters to confirm its immunotoxic effects in dogs. Further studies are required to investigate the toxic effects of ZnO NPs using other routes of exposure such as inhalation, ingestion, and parentral injections in dogs despite using fewer doses for a longer time of exposure to study the possible chronic toxicity of NPs exposure in dogs.

Conclusion

It was concluded that the daily subcutaneous injections of dogs with 50 and 100 ppm ZnO NPs caused extensive systemic toxicity. It caused notable disturbances in the hematological parameters and increased levels of liver and kidney biomarkers. The histopathological alterations of ZnO NPs on most organs, including the liver, kidneys, lungs, spleen, and heart are dose-dependent. Despite the fact that ZnO NPs cause oxidative stress, other pathological processes, such as inflammation and apoptosis, have been connected to the pathophysiology of ZnO NPs in dogs. ZnO NPs increased the expression of the apoptotic marker caspase-3, upregulated both proinflammatory cytokine TNFα and angiogenic factor VEGFA, and downregulated the anti-inflammatory mediator IL-10.

Acknowledgements
Not applicable.

Author contributions
M.H.H, H.F and E.I.H conceived the study, designed the experiment, written the first draft of the manuscript, reviewed all the results. M.H.H, I.A.E and H.F performed the experiment, physical examinations, radiological and ultrasonographic examinations. M.A.I. performed the molecular study. N.H.H performed the hematological examination, biochemical analysis, and oxidative stress evaluations. K.Y.F prepared and identified ZnO NPs. E.I.H performed histopathological analysis and immunohistochemistry. All authors wrote, read, revised, and approved the final manuscript.

Funding
This research didn't receive any specific grant from funding agencies in the public, commercial, or not-for-profit sectors.

Data availability
The datasets used and/or analysed during the current study are available from the corresponding author on reasonable request.

Declarations

Ethics approval and consent to participate
All experimental procedures were conducted following the ARRIVE guidelines for the experimental research on animals (PLoS Bio 8(6), e1000412,2010), and approved by the Institutional Animal Care and Use Committee of Cairo University (IACUC), approval number; CU/F/40/23. The study was conducted in accordance with relevant guidelines and regulations. All dogs' owners were aware that their animals will be included in research purposes and signed a written consent indicating their approval.

Consent for publication
Not applicable.

Competing interests
The authors declare no competing interests.

Received: 13 June 2024 / Accepted: 4 September 2024
Published online: 18 October 2024

References

1. Farooqi ZUR, Qadeer A, Hussain MM, Zeeshan N, Ilic P. Characterization, and physicochemical properties of nanomaterials. In Nanomaterials: Synthesis, Characterization, Hazards, and Safety; Elsevier: 2021, 97–121, https://doi.org/10.1016/C2020-0-00287-2
2. Salem SS, Fouda A, Green. Synthesis of metallic nanoparticles and their prospective biotechnological applications: an overview. Biol Trace Elem Res. 2021;199:344–70. https://doi.org/10.1007/s12011-020-02138
3. Raeeszadeh M, Karimfar B, Amiri AA, Akbari A. Protective effect of nano-vitamin C on infertility due to oxidative stress induced by lead and arsenic in male rats. J Chem. 2021;2021(1):9589345.
4. Ashe B. A detail investigation to observe the effect of zinc oxide and silver nanoparticles in biological system. M.Sc. (Roll NO-607bm004). National Institute of Technology; 2011.
5. Sahoo S. Socio-ethical issues, and nanotechnology development: perspectives from India, in 2010 10th IEEE Conference on Nanotechnology (IEEE-NANO), Seoul, South Korea, USA, 17–20 August 2010 (IEEE, 2010), pp. 1205–1210. https://doi.org/10.1109/NANO.2010.5697887
6. Hassanen EI, Morsy EA, Abuowarda M, et al. Silver and gold nanoparticles as a novel approach to fight Sarcoptic mange in rabbits. Sci Rep. 2024;14:10618. https://doi.org/10.1038/s41598-024-60736-w
7. El-Naggar ME, Hasanin M, Hashem AH. Eco-friendly synthesis of superhydrophobic antimicrobial film based on cellulose acetate/polycaprolactone loaded with the green biosynthesized copper nanoparticles for food packaging application. J Polym Environ. 2021. https://doi.org/10.1007/s10924-021-02318-9
8. Jiang J, Pi J, Cai J. The advancing of zinc oxide nanoparticles for biomedical applications. Bioinorg. Chem Appl. 2018;5:1–18. https://doi.org/10.1155/2018/ 10625 62 (2018).
9. Vijayaram S, Razafindralambo H, Sun YZ, Vasantharaj S, Ghafarifarsani H, Hoseinifar SH, Raeeszadeh M. Applications of green synthesized metal nanoparticles - a review. Biol Trace Elem Res. 2024;202(1):360–86. https://doi.org/10.1007/s12011-023-03645-9. Epub 2023 Apr 13. PMID: 37046039; PMCID: PMC10097525.
10. Hassanen EI, Ragab EI. Vivo and in vitro assessments of the antibacterial potential of chitosan-silver nanocomposite against methicillin-resistant *Staphylococcus aureus*–induced infection in rats. Biol Trace Elem Res. 2021;199:244–257. Published in 18 April 2020. https://doi.org/10.1007/s12011-020-02143-6
11. Seil JT, Webster TJ. Antimicrobial applications of nanotechnology: methods and literature. Int J Nanomed. 2012;7:2767–81. https://doi.org/10.2147/IJN.S24805
12. Manuja A. Zinc oxide nanoparticles: opportunities and challenges in veterinary sciences. Immunome Res. 2015;11(2). https://doi.org/10.4172/1745-7580.1000095
13. Manuja A, Kumar B, Singh RK. Nanotechnology developments: opportunities for animal health and production. Nanatechnol Dev. 2012;2:17–25.
14. Fedota N, Gorchakov E, Bagamaev B, Kireev I, Shahova V, Kolodkin V. (2019). Local treatment of burn wounds in animals using a new nanocomponent ointment. In *E3S Web of Conferences* (Vol. 135, p. 01084). EDP Sciences.
15. Abd-El Azeem RM, Ibrahim A, Kotob MH, Elshahawy A, Selim SM. Evaluation of the healing of wounds dressed with zinc metal-organic frameworks (Zn-MOFs) in dogs: an experimental study. Assiut Veterinary Med J. 2022;68(175):139–59.
16. McFadden RA, Heinrich NA, Haarstad AC, Tomlinson DJ. A double-blinded, randomized, controlled, crossover evaluation of a zinc methionine supplement as an adjunctive treatment for canine atopic dermatitis. Vet Dermatol. 2017;28:569–e138.
17. Khanipour Machiani M, Jamshidi S, Nikaein D, Khosravi A, Balal A. The inhibitory effects of zinc oxide nanoparticles on clinical isolates of microsporum canis in dogs and cats. Veterinary Med Sci. 2024;10(1):e1316.
18. Viswanathan K, Vaiyamalai R, Bharathi babu D, Priyadharshini M, Raman ML, M., Dhinakarraj G. Ketoconazole-conjugated ZnO nanoparticles based semi-solid formulation and study their impacts on skin disease. IET Nanobiotechnol. 2018;12(8):1097–101.
19. Sahoo RK, Rani S, Kumar V, Gupta U. Zinc oxide nanoparticles for bioimaging and drug delivery. Nanostructured Zinc Oxide. Elsevier; 2021. pp. 483–509.
20. Zoufan P, Baroonian M, Zargar B. ZnO nanoparticles-induced oxidative stress in Chenopodium murale L, zn uptake, and accumulation under hydroponic culture. Environ Sci Pollut Res. 2020;27:11066–78.
21. Kao YY, Chen YC, Cheng TJ, Chiung YM, Liu PS. Zinc oxide nanoparticles interfere with zinc ion homeostasis to cause cytotoxicity. Toxicol Sci. 2012;125:462–72.
22. Cheng WY, Tong H, Miller EW, Chang CJ, Remington J, et al. An integrated imaging approach to the study of oxidative stress generation by mitochondrial dysfunction in living cells. Environ Health Perspect. 2010;118:902–8.

23. Chiang HM, Xia Q, Zou X, Wang C, Wang S, et al. Nanoscale ZnO induces cytotoxicity and DNA damage in human cell lines and rat primary neuronal cells. J Nanosci Nanotechnol. 2012;12:2126–35.
24. Sharma V, Singh P, Pandey AK, Dhawan A. Induction of oxidative stress, DNA damage and apoptosis in mouse liver after sub-acute oral exposure to zinc oxide nanoparticles. Mutat Res. 2012;745:84–91.
25. Yi J, Li Y, Mai Q, Li Y, Lin Y, Weng X, Ai Z, Li M, Shang P, Iqbal M, Mehmood K, Chang Y-F, Tang Z, Zhang H, Li Y. Hepatotoxicity and the role of the gut–liver axis in dogs after oral administration of zinc oxide nanoparticles. Metallomics. 2022;14(11). https://doi.org/10.1093/mtomcs/mfac066
26. Kumar SS, Venkateswarlu P, Rao VR, Rao GN. Synthesis, characterization and optical properties of zinc oxide nanoparticles. Int Nano Lett. 2013;3(30):1–6.
27. Negahdary M, Chelongar R, Zadeh SK, Ajdary M. The antioxidant effects of silver, gold, and zinc oxide nanoparticles on male mice in in vivo condition. Adv Biomed Res. 2015;4:69. https://doi.org/10.4103/2277-9175.153893. PMID: 25878994; PMCID: PMC4386201.
28. Chuang HC, Chuang KJ, Chen JK, Hua HE, Shen YL, Liao WN, Cheng TJ. Pulmonary pathobiology induced by zinc oxide nanoparticles in mice: a 24-hour and 28-day follow-up study. Toxicol Appl Pharmcol. 2017;327:13–22.
29. Barrett KE, B. S. Ganong's review of medical physiology. Volume 25. th). McGraw-Hill Education; 2016.
30. Bain BJ, Bates I, Laffan MA. Dacie and Lewis practical haematology e-book. Elsevier Health Sciences; 2016.
31. Aziz RLA, Abdel-Wahab A, Abdel-Razik AH, Kamel S, Farghali AA, Saleh R, Mahmoud R, Ibrahim MA, Nabil TM, El-Ela FIA. Physiological roles of propolis and red ginseng nanoplatforms in alleviating dexamethasone-induced male reproductive challenges in a rat model. Mol Biol Rep. 2024;51(1):72. https://doi.org/10.1007/s11033-023-08991-4
32. Farid MF, Abouelela YS, Yasin NAE, Al-Mokaddem AK, Prince A, Ibrahim MA, Rizk H. Laser-activated autologous adipose tissue-derived stromal vascular fraction restores spinal cord architecture and function in multiple sclerosis cat model. Stem Cell Res Ther. 2023;14(1):6. https://doi.org/10.1186/s13287-022-03222-2
33. Bancroft J, Gamble M. Theory and practice of histological techniques. In: Bancroft J, editor. Churchill Livingstone. Oxford: Elsevier; 2013.
34. Hassanen EI, Hussien AM, Mehanna S, et al. Comparative assessment on the probable mechanisms underlying the hepatorenal toxicity of commercial imidacloprid and hexaflumuron formulations in rats. Environ Sci Pollut Res. 2022;29:29091–104. https://doi.org/10.1007/s11356-021-18486-z
35. Hassanen EI, Kamel S, Mohamed WA, Mansour HA, Mahmoud MA. The potential mechanism of histamine-inducing cardiopulmonary inflammation and apoptosis in a novel oral model of rat intoxication. Toxicology. 2023a;484:153410. https://doi.org/10.1016/j.tox.2022.153410
36. Hassanen EI, Morsy EM, Hussien AM, Ibrahim MA, Farroh KY. The effect of different concentrations of gold nanoparticles on growth performance, toxicopathological and immunological parameters of broiler chickens. Biosci Rep. 2020;40(3):BSR20194296. https://doi.org/10.1042/BSR20194296
37. Hussain I, Singh NB, Singh A, Singh H, Singh SC. Green synthesis of nanoparticles and its potential application. Biotechnol Lett. 2016;38:545–60. https://doi.org/10.1007/s10529-015-2026-7
38. Khalaf AA, Hassanen EI, Azouz RA, et al. Ameliorative effect of zinc oxide nanoparticles against dermal toxicity induced by lead oxide in rats. Int J Nanomed 20 September. 2019;14:7729–41. https://doi.org/10.2147/IJN.S2
39. Hassanen EI, Morsy EA, Hussien AA, Farroh KY, Ali ME. Comparative assessment of the bactericidal effect of nanoparticles of copper oxide, silver, and chitosan-silver against *Escherichia coli* infection in broilers. Biosci Rep. 2021;30(4):BSR20204091. https://doi.org/10.1042/BSR20204091
40. Englar RE. Performing the Small Animal Physical Examination. 1st ed. wiley Blackwell; 2017.
41. Schär M. Clinical medicine of the dog and cat, 2nd ed., 2009, M.anson publishing.
42. Stellato AC, Dewey CE, Widowski TM, Niel L. Evaluation of associations between owner presence and indicators of fear in dogs during routine veterinary examinations. J Am Vet Med Assoc. 2020;257(10):1031–40.
43. Ebedy YA, Elshazly MO, Hassan NH, Ibrahim MA, Hassanen EI. Novel insights into the potential mechanisms underlying carbendazim-induced hepatorenal toxicity in rats. J Biochem Mol Toxicol. 2022;36:e23079. https://doi.org/10.1002/jbt.23079
44. Mo E, Ebedy YA, Ibrahim MA, Farroh KY, Hassanen EI. Newly synthesized chitosan-nanoparticles attenuate carbendazim hepatorenal toxicity in rats via activation of Nrf2/HO1 signalling pathway. Sci Rep. 2022;12(1):9986. https://doi.org/10.1038/s41598-022-13960-1
45. Khalaf AAA, Elhady M, Hassanen EI, Azouz AA, Ibrahim MA, Galal M, Noshy PA, Azouz RA. Antioxidant role of carvacrol against hepatotoxicity and nephrotoxicity induced by propiconazole in rats. Rev Bras Farmacogn. 2021;31:1–8.
46. Chen CB, Hammo B, Barry J, Radhakrishnan K. Overview of albumin physiology and its role in pediatric diseases. Curr Gastroenterol Rep. 2021;23(8):11. https://doi.org/10.1007/s11894-021-00813-6
47. Brookes EM. and David A. Power. Elevated serum urea-to-creatinine ratio is associated with adverse inpatient clinical outcomes in non-end stage chronic kidney disease. Scientific reports. 2022;12(1):20827.
48. Almansour M, Alarifi S, Melhim W, Jarrar BM. Nephron ultrastructural alterations induced by zinc oxide nanoparticles: an electron microscopic study. IET Nanobiotechnol. 2019;13(5):515–21. https://doi.org/10.1049/iet-nbt.2018.5219
49. Stern ST, Adiseshaiah PP, Crist RM. Autophagy and lysosomal dysfunction as emerging mechanisms of nanomaterial toxicity. Part Fibre Toxicol. 2012;9(1):20. https://doi.org/10.1186/1743-8977-9-20
50. Aboulhoda BE, Abdeltawab DA, Rashed LA, Abd Alla MF, Yassa HD. Hepatotoxic effect of oral zinc oxide nanoparticles and the ameliorating role of selenium in rats: a histological, immunohistochemical and molecular study. Tissue Cell. 2020;67:101441. https://doi.org/10.1016/j.tice.2020.101441
51. Pei X, Tang S, Jiang H, Zhang W, Xu G, Zuo Z, Ren Z, Chen C, Shen Y, Li C, Li D. Paeoniflorin recued hepatotoxicity under zinc oxide nanoparticles exposure via regulation on gut-liver axis and reversal of pyroptosis. Sci Total Environ. 2023;904:166885. https://doi.org/10.1016/j.scitotenv.2023.166885
52. Pei X, Jiang H, Xu G, Li C, Li D, Tang S. Lethality of zinc oxide nanoparticles surpasses conventional zinc oxide via oxidative stress, mitochondrial damage and calcium overload: a comparative hepatotoxicity study. Int J Mol Sci. 2022;23(12):6724.
53. Abou-Zeid SM, Zheng C, Khalil SR, Farag MR, Elsabbagh HS, Siddique MS, Mawed SA, Azzam MM, Di Cerbo A, Elkhadrawey BA. Thymol-enriched diet alleviates the toxic impacts of zinc oxide nanoparticles on growth performance, blood biochemistry, oxidant/antioxidant status and stress-related genes and histology of liver and gills in Oreochromis niloticus. Aquaculture Rep. 2023;33:101750. https://doi.org/10.1016/j.aqrep.2023.101750
54. Kausar S, Jabeen F, Latif MA, Asad M. Characterization, dose dependent assessment of hepatorenal oxidative stress, hematological parameters and histopathological divulging of the hepatic damages induced by zinc oxide nanoparticles (ZnO-NPs) in adult male Sprague Dawley rats. Saudi J Biol Sci. 2023;30(9):103745. https://doi.org/10.1016/j.sjbs.2023.103745
55. Xiao L, Liu C, Chen X, Yang Z. Zinc oxide nanoparticles induce renal toxicity through reactive oxygen species. Food Chem Toxicol. 2016;90:76–83. https://doi.org/10.1016/j.fct.2016.02.002
56. Ghareeb OA. Toxicopathological effects of zinc oxide nanoparticles on the liver function and preventive role of silymarin in vivo. Indian J Forensic Med Toxicol. 2021;15(2):3212–7.
57. Hassanen EI, Abdelrahman RE, Aboul-Ella H, et al. Mechanistic approach on the pulmonary oxido-inflammatory stress induced by cobalt ferrite nanoparticles in rats. Biol Trace Elem Res. 2023b. https://doi.org/10.1007/s12011-023-03700-5
58. Raguvaran R, Manuja A, Manuja BK. Zinc oxide nanoparticles: opportunities and challenges in veterinary sciences. Immunome Res. 2015;11:95. https://doi.org/10.4172/1745-7580.1000095
59. Baek M, Chung HE, Yu J, Lee JA, Kim TH, Oh JM, Lee WJ, Paek SM, Lee JK, Jeong J, Choy JH, Choi SJ. Pharmacokinetics, tissue distribution, and excretion of zinc oxide nanoparticles. Int J Nanomed. 2012;7:3081–97. https://doi.org/10.2147/IJN.S32593. Epub 2012 Jun 26. PMID: 22811602; PMCID: PMC3394467.
60. Fujihara J, Tongu M, Hashimoto H, Yamada T, Kimura-Kataoka K, Yasuda T, Fujita Y, Takeshita H. Distribution and toxicity evaluation of ZnO dispersion nanoparticles in single intravenously exposed mice. J Med Invest. 2015;62(1–2):45–50. https://doi.org/10.2152/jmi.62.45
61. Li C-H, Shen C-C, Cheng Y-W, Huang S, Wu C-C, Kao C-C, Liao J-W, Kang, Jaw-Jou. Organ biodistribution, clearance, and genotoxicity of orally administered zinc oxide nanoparticles in mice. Nanotoxicology. 2011;6:746–56. https://doi.org/10.3109/17435390.2011.620717
62. Pei X, Jiang H, Li C, Li D, Tang S. Oxidative stress-related canonical pyroptosis pathway, as a target of liver toxicity triggered by zinc oxide nanoparticles. J Hazard Mater. 2023;442:130039.
63. Liu Z, Lv X, Xu L, Liu X, Zhu X, Song E, Yang Song. Zinc oxide nanoparticles effectively regulate autophagic cell death by activating autophagosome formation and interfering with their maturation. Part Fibre Toxicol. 2020;17:1–17.

64. Aboulhoda, Emad B, Abdeltawab DA, Rashed LA, Alla MFA and Yassa HD. Hepatotoxic effect of oral zinc oxide nanoparticles and the ameliorating role of selenium in rats: a histological, immunohistochemical and molecular study. Tissue Cell. 2020;67:101441.
65. Esmaeillou M, Moharamnejad M, Hsankhani R, Tehrani AA, Maadi H. Toxicity of ZnO nanoparticles in healthy adult mice. Environ Toxicol Pharmacol. 2013;35:67–71.
66. Ansari MA, Khan HM, Khan AA, Alzohairy MA. Biochemical and histopathological ultrastructural changes caused by ZnO nanoparticles in mice. Toxicol Environ Chem. 2015:1–16. https://doi.org/10.1080/02772248.2015.1077960
67. Sharma V, Anderson D, Dhawan A. Zinc oxide nanoparticles induce oxidative DNA damage and ROS-triggered mitochondria mediated apoptosis in human liver cells (HepG2). Apoptosis. 2012;17(8):852–70. https://doi.org/10.1007/s10495-012-0705-6
68. Ansar S, Abudawood M, Alaraj ASA, Hamed SS. Hesperidin alleviates zinc oxide nanoparticle induced hepatotoxicity and oxidative stress. BMC Pharmacol Toxicol. 2018;19(1):65. https://doi.org/10.1186/s40360-018-0256-8
69. Guo T, Fang X, Liu Y, Ruan Y, Hu Y, Wang X, Hu Y, Wang G, Xu Y. Acute lung inflammation induced by zinc oxide nanoparticles: evolution and intervention via NRF2 activator. Food Chem Toxicol. 2022;162:112898. https://doi.org/10.1016/j.fct.2022.112898
70. Zhuo L-B, Liu Y-M, Jiang Y, Yan Z. Zinc oxide nanoparticles induce acute lung injury via oxidative stress-mediated mitochondrial damage and NLRP3 inflammasome activation: in vitro and in vivo studies. Environ Pollut. 2024;341:122950. https://doi.org/10.1016/j.envpol.2023.122950
71. Ng CT, Yong LQ, Hande MP, Ong CN, Yu L, Bay BH, Baeg GH. Zinc oxide nanoparticles exhibit cytotoxicity and genotoxicity through oxidative stress responses in human lung fibroblasts and drosophila melanogaster. Int J Nanomed. 2017;12:1621–37. https://doi.org/10.2147/IJN.S124403
72. Liu S, Zhou H, Shi Y, Yi S, Wang X, Li J, Liao B, Cao J, Li G. Zinc oxide nanoparticles induce renal injury by initiating oxidative stress, mitochondrial damage and apoptosis in renal tubular epithelial cells. Biol Trace Elem Res. 2024;202(2):481–92. https://doi.org/10.1007/s12011-023-03683-3
73. Sahu D, Kannan GM, Vijayaraghavan R, Anand T, Khanum F. Nanosized zinc oxide induces toxicity in human lung cells. ISRN Toxicol. 2013;2013:1–8. https://doi.org/10.1155/2013/316075
74. Ali AA, Tamimi SQ, Maliki SJ, Abdullah MA. Toxic effects of zinc oxide nanoparticles and histopathological and caspase-9 expression changes in the liver and lung tissues of male mice model. Appl Nanosci. 2022:1–11.
75. Saman S, Saeed M, Attaollah S, Masoud G. Histopathological effects of ZnO nanoparticles on liver and heart tissues in Wistar rats. Adv Biores. 2013;4(2):83–8.
76. Mohammed H, El Shakaa N, Bahaa N, Abo Zeid A. A histological study on the acute effect of zinc oxide nanoparticles administered by different routes on albino rat lung. 2022;10(2):72–80.
77. Mohammad GRKS, Seyedi SMR, Karimi E, Homayouni-Tabrizi M. The cytotoxic properties of zinc oxide nanoparticles on the rat liver and spleen, and its anticancer impacts on human liver cancer cell lines. J Biochem Mol Toxicol. 2019;e22324:1–9. https://doi.org/10.1002/jbt.22324
78. Lee AR, Lee SJ, Lee M, Nam M, Lee S, Choi J, Lee HJ, Kim DU, Hoe KL. Editor's highlight: a genome-wide screening of target genes against silver nanoparticles in fission yeast. Toxicol Sci. 2018;161:171–185.
79. Pandey A, Mishra AK. Immunomodulation, toxicity, and therapeutic potential of nanoparticles. BioTech. 2022;11(3):42. https://doi.org/10.3390/biotech11030042
80. Liu Y, Hardie J, Zhang X, Rotello VM. Effects of engineered nanoparticles on the innate immune system. Semin Immunol. 2017;34:25–32.
81. Senapati VA, Gupta GS, Pandey AK, Shanker R, Dhawan A, Kumar A. Zinc oxide nanoparticle induced age dependent immunotoxicity in BALB/c mice. Toxicol Res. 2017;6(3):342–52.
82. Zolnik BS, Gonzalez-Fernandez A, Sadrieh N, Dobrovolskaia MA. Nanoparticles and the immune system. Endocrinology. 2010;151:458–65.
83. Alkaladi A, El-Deen NAMN, Afifi M, Zinadah OAA. Hematological and biochemical investigations on the effect of vitamin E and C on Oreochromis niloticus exposed to zinc oxide nanoparticles. Saudi J Biol Sci. 2015;22(5):556–63. https://doi.org/10.1016/j.sjbs.2015.02.012
84. Fadl F, Hassan A, Abdelaziz M, Aita NAA, Amira Mohamed H. Mohamed. Ameliorative effect of Zinc Oxide nanoparticles against Streptococcus parauberis experimental infection in Nile Tilapia (Oreochromis niloticus). Egypt J Veterinary Sci. 2024;55(7):2025–54.
85. Srivastav AK, Kumar M, Ansari NG, Jain AK, Shankar J, Arjaria N, Jagdale P, Singh D. A comprehensive toxicity study of zinc oxide nanoparticles versus their bulk in Wistar rats. Hum Exp Toxicol. 2016;35(12):1286–304. https://doi.org/10.1177/0960327116629530
86. Abass MA, Selim SA, Selim AO, El-Shal AS, Gouda ZA. Effect of orally administered zinc oxide nanoparticles on albino rat thymus and spleen. IUBMB Life. 2017;69(7):528–39. https://doi.org/10.1002/iub.1638
87. Harvey JW. (2012). Evaluation of leukocytic disorders. In Veterinary Hematology (pp. 122–176). Elsevier. https://doi.org/10.1016/B978-1-4377-0173-9.00005-1
88. Alghsham RS, Satpathy SR, Bodduluri SR, Hegde B, Jala VR, Twal W, Burlison JA, Sunkara M, Haribabu B. Zinc oxide nanowires exposure induces a distinct inflammatory response via CCL11-mediated eosinophil recruitment. Front Immunol. 2019;10. https://doi.org/10.3389/fimmu.2019.02604
89. Wang J, Deng X, Zhang F, Chen D, Ding W. ZnO nanoparticle-induced oxidative stress triggers apoptosis by activating JNK signaling pathway in cultured primary astrocytes. Nanoscale Res Lett. 2014;9:117.
90. Shen J, Yang D, Zhou X, Wang Y, Tang S, Yin H, Wang J, Chen R, Chen J. Role of autophagy in zinc oxide nanoparticles-induced apoptosis of mouse LEYDIG cells. Int J Mol Sci. 2019;20(16):4042.
91. Wilhelmi V, et al. Zinc oxide nanoparticles induce necrosis and apoptosis in macrophages in a p47phox- and Nrf2-independent manner. PLoS ONE. 2013;8(6):e65704.
92. Hassanen EI, Tohamy AF, Hassan AM, Ibrahim MA, Issa MY, Farroh KY. Pomegranate juice diminishes the mitochondrial-dependent cell death and NF-κB signaling pathway induced by copper oxide nanoparticles on the liver and kidneys of rats. Int J Nanomed 15 November. 2019;14:8905–22.
93. AbdElrazek DA, Ibrahim MA, Hassan NH, Hassanen EI, Farroh KY, Abass HI. Neuroprotective effect of quercetin and nano-quercetin against cyclophosphamide-induced oxidative stress in the rat brain: role of Nrf2/ HO-1/Keap-1 signaling pathway. Neurotoxicology. 2023. ISSN 0161-813X https://doi.org/10.1016/j.neuro.2023.06.008
94. Morgan AM, Hassanen EI, Ogaly HA, Al Dulmani SA, Al-Zahrani FAM, Galal MK, Kamel S, Rashad MM, Ibrahim MA, Hussien AM. J. The ameliorative effect of N-acetylcysteine against penconazole induced neurodegenerative and neuroinflammatory disorders in rats. Biochem Mol Toxicol. 2021;e22884. https://doi.org/10.1002/jbt.22884
95. Wang B-J, Chen Y-Y, Chang H-H, Chen R-J, Wang Y-J. Zinc oxide nanoparticles exacerbate skin epithelial cell damage by upregulating pro-inflammatory cytokines and exosome secretion in M1 macrophages following UVB irradiation-induced skin injury. Part Fibre Toxicol. 2024;21(1):9.
96. Faddah LM, Baky NAA, Al-Rasheed NM, Al-Rasheed NM, Fatani AJ, Atteya M. Role of quercetin and arginine in ameliorating nano zinc oxide-induced nephrotoxicity in rats. BMC Complement Altern Med. 2012;12(1):1062.
97. Fukai T. and Masuko Ushio-Fukai. Cross-talk between NADPH oxidase and mitochondria: role in ROS signaling and angiogenesis. Cells. 2020;9(8):1849.

Publisher's note